

wave functions. However, the  $f_s$  values calculated with either of the wave functions are not unreasonable. The  $f_s$  values for O<sup>17</sup> are in agreement with those calculated by O'Reilly and Tsang,<sup>3</sup> who used HF wave functions for the O<sup>2-</sup> ion.

The important result is to note that with the measured  $A^{33}$  the  $f_s$  values for S<sup>33</sup> are approximately the same as those for O<sup>17</sup> and Se<sup>77</sup>. This is expected because of the similarity in the crystallographic and magnetic prop-

erties of these cubic antiferromagnets. Therefore, the relatively small value for  $A^{33}$  is reasonable and consistent with the theoretical calculations.

#### ACKNOWLEDGMENTS

The author would like to thank Dr. E. D. Jones, not only for providing the sample but also for enlightening discussions, and Dr. J. R. Morton for the wave-function calculations.

### Stopping Powers of S<sup>32</sup>, Cl<sup>35</sup>, Br<sup>79</sup>, and I<sup>127</sup> Ions in Mylar\*

T. E. PIERCE, W. W. BOWMAN, AND MARSHALL BLANN

*Department of Chemistry and Nuclear Structure Research Laboratory, University of Rochester, Rochester, New York*

(Received 7 March 1968)

Stopping powers of Mylar are presented for S<sup>32</sup> ions of mean energy 15 to 95 MeV, Cl<sup>35</sup> ions of 15 to 95 MeV, Br<sup>79</sup> ions of 30 to 90 MeV, and I<sup>127</sup> ions of 60 and 105 MeV. The heavy-ion beams were accelerated on the Rochester MP tandem Van de Graaff; energies were known to  $\pm 50$  keV. The precision of energy-loss measurements was of the order of 2% with an estimated accuracy of  $\pm 8\%$ . The experimentally determined stopping powers were used with the Bethe-Bloch equation and experimental proton stopping powers to calculate effective charges. The fractional effective charges for the ions investigated all fit a single smooth curve when compared with a reduced velocity variable; published values for O<sup>16</sup>-ion stopping powers in carbon and aluminum yielded effective charges which fit the same curve. The effective charges for S<sup>32</sup>, Br<sup>79</sup>, and I<sup>127</sup> are compared with the experimental most probable charge states, and are found to be less than the experimental values in all cases. This variation at its greatest is found to be 67%.

#### INTRODUCTION

**T**HEORIES of heavy-ion stopping for ions of a few MeV to  $\sim 100$  MeV have met with limited success.<sup>1,2</sup> With a paucity of experimental stopping powers for heavy ions, and no satisfactory theory, there is a need for more data and a semiempirical means of correlating the available data, so that interpolations and extrapolations may be performed with reasonable accuracy.

Recently, Cumming and Crespo presented stopping-power data for light and heavy fission fragments in Mylar, and investigated several semiempirical means of correlating these data.<sup>3</sup> In this paper, we present stopping powers in Mylar for S<sup>32</sup>, Cl<sup>35</sup>, Br<sup>79</sup>, and I<sup>127</sup> ions at energies between 15 and 105 MeV. We use these data to test further a mode of correlation used for heavy-ion data in Ref. 3 and elsewhere.<sup>4,5</sup> The data are of interest for several reasons, among them the

similarity in composition of Mylar (C<sub>10</sub>H<sub>8</sub>O<sub>4</sub>) to tissue,<sup>6</sup> the use of Mylar as a degrader in many nuclear recoil studies,<sup>7</sup> and as an aid in interpretation of ion-track registration sensitivities of some nuclear-track detectors.<sup>8</sup>

#### EXPERIMENTAL

The heavy-ion beams used in this work were accelerated on the Rochester MP tandem Van de Graaff accelerator. All beams were extracted from the hydrogen duoplasmatron source using  $\sim 5\%$  impurities of H<sub>2</sub>S, HBr, or HI; or in the case of chlorine, the beam was produced from several milligrams of solid NH<sub>4</sub>Cl placed in the source. Terminal voltages up to 10 MV were used, with only single-charge states being passed around the 90° analyzing magnet. The machine was stabilized on an analyzed current of  $\leq 5$  nA. A switching magnet following the analyzer was used to deflect the beam another 45° into the "chemistry" beam line. Approximately 6 m from the switching magnet, there was a 3 mm aperture in the line, behind which was a solid-

\* This work was supported by the U.S. Atomic Energy Commission.

<sup>1</sup> J. Lindhard, M. Scharff, and H. E. Schiott, Kgl. Danske Videnskab. Selskab, Mat. Fys. Medd. **33**, No. 14 (1963).

<sup>2</sup> L. C. Northcliffe, Ann. Rev. Nucl. Sci. **13**, 67 (1963).

<sup>3</sup> J. B. Cumming and V. P. Crespo, Phys. Rev. **161**, 287 (1967).

<sup>4</sup> W. Booth and I. S. Grant, Nucl. Phys. **63**, 481 (1965).

<sup>5</sup> P. G. Roll and F. E. Steigert, Phys. Rev. **120**, 470 (1960).

<sup>6</sup> P. E. Schambra, A. M. Rauth, and L. C. Northcliffe, Phys. Rev. **120**, 1758 (1960).

<sup>7</sup> J. M. Alexander, in *Nuclear Chemistry*, edited by L. Yaffe (Academic Press Inc., New York, 1968).

<sup>8</sup> R. L. Fleischer, P. B. Price, R. M. Walker, and E. L. Hubbard, Phys. Rev. **156**, 353 (1967); P. B. Price (private communication).

TABLE I. Stopping powers in Mylar for S<sup>32</sup>, Cl<sup>35</sup>, Br<sup>79</sup>, and I<sup>127</sup> ions.

Projectile	Mean energy (MeV)	$\Delta E/\Delta X$ (MeV)	$\Delta E/\Delta X$ (keV/ $\mu\text{g cm}^2$ )	Mylar thickness ( $\mu\text{g/cm}^2$ )
S <sup>32</sup>	75.0	10.1	19.0	529
	64.8	10.5	19.8	
	54.6	10.8	20.5	
	44.3	11.4	21.6	
	34.0	11.9	22.6	
	23.8	12.4	23.4	
	14.1	11.9	22.8	
S <sup>32</sup>	96.7	6.6	19.5 <sup>a</sup>	335
	76.6	6.8	20.5 <sup>a</sup>	
	56.3	7.4	22.4 <sup>a</sup>	
	35.8	8.4	25.2 <sup>a</sup>	
	15.5	9.1	26.7 <sup>a</sup>	
Cl <sup>35</sup>	96.5	7.1	21.1	335
	76.3	7.4	22.1	
	56.0	7.9	23.7	
	35.7	8.6	25.8	
	15.7	8.7	25.9	
Br <sup>79</sup>	89.6	20.8	62.1	335
	59.8	20.4	61.0	
	31.4	17.2	51.4	
I <sup>127</sup>	105	30.0	90	335
	57.9	24.2	72	

<sup>a</sup> Average of two determinations; the deviation about the mean was typically  $\pm 6\%$ .

state radiation detector (ORTEC fission-fragment detector). The detector was calibrated by successively allowing single-charge-state components (energies) of the beam to hit the detector. This was repeated for each ion until six to eight calibration energies between 10 and 110 MeV were recorded. Pulse-height spectra of 2048 channels were collected. Pulsers were run with all spectra to check against drift; there was none ( $\leq 50$  keV at 100 MeV). Counting rates were regulated to be between 10 and 100 pulses per second by careful adjustment of the current through the switching magnet, with defocusing of the quadrupole triplet preceding the switching magnet. The calibration points were fitted by least-square analyses, with no points relevant to this work being more than 200 keV off the line. The beam energies were known to  $\pm 50$  keV or better (this figure assumes a  $\pm 5$  keV terminal stabilization figure).

After calibrating the pulse-height-versus-energy response for the detector for the ion being used, a Mylar window was placed between the detector and the 3-mm aperture. Some of the ion energies used in calibration were again allowed to hit the detector, giving the degraded energies through the Mylar window.

In earlier experiments quarter-mil aluminized Mylar windows were used, of total thickness 529  $\mu\text{g/cm}^2$ . This figure includes approximately 20- $\mu\text{g/cm}^2$  aluminum, which was ignored in computing  $\Delta E/\Delta X$ . Later experiments used 335- $\mu\text{g/cm}^2$  Mylar;  $\sim 5$   $\mu\text{g/cm}^2$  of gold was vacuum-evaporated onto the Mylar after weighing. This was also neglected in calculating  $\Delta E/\Delta X$ , i.e., it

was assumed that the windows were 335- $\mu\text{g/cm}^2$  Mylar with no other substance on them. For accuracies involved in this work, and considering the relative stopping powers of Mylar, aluminum, and gold, we feel that this is a reasonable way to treat the data.<sup>9</sup> The results of these measurements are summarized in Table I. Mylar thicknesses were determined by weighing known areas on a microbalance; different portions of 6 $\times$ 6-in. Mylar sheets gave thicknesses consistent to within 1%. While the average thicknesses are thus uniform to 1%, we cannot be certain that a microscopic variation does not exist. From the broadening of the detector pulse-height response for heavy ions passing through the Mylar windows, we estimate an upper limit of  $\pm 4\%$  for errors due to microscopic nonuniformity. Considering all sources of uncertainty, we estimate an error of  $\pm 8\%$  for the data of Table I. This error estimate should include differences between  $\Delta E/\Delta X$  and  $dE/dX$ .

## RESULTS AND DISCUSSION

Energy-loss relationships for light ions ( $A \leq 4$ ) which are completely stripped are generally based on some form of the Bethe-Bloch equation<sup>10</sup>

$$(dE/dX)_e \propto (Z_1^2 Z_2 / v^2 A_2) \ln(2mv^2/I), \quad (1)$$

where  $Z_1$  represents the atomic number of projectile,  $Z_2$  and  $A_2$  represent the atomic number and mass number of the stopping medium, and the subscript  $e$  denotes electronic stopping. The logarithmic term is a function solely of the nature of the stopping medium and of the velocity of the projectile. Heavy ions present a difficulty with respect to Eq. (1) in that they are only partially ionized in the energy range of interest to much of heavy-ion physics. This had led many<sup>2-4,6</sup> who have studied heavy-ion stopping phenomena to look for a smooth function relating an "effective charge" to a reduced ion velocity where the effective charge is the value which gives the correct  $(dE/dX)_e$  in Eq. (1), and the reduced velocity is often taken as the ratio of the velocity  $v$  to the Thomas-Fermi electron velocity  $v_0 Z_1^{2/3}$ , where  $v_0 = e^2/\hbar$ . This has been done by substituting  $\gamma_1 Z_1 = Z_{\text{eff}}$  for  $Z_1$  in Eq. (1), and comparing with proton stopping powers for protons of the same velocity and in the same stopping medium. This may be represented by

$$\frac{(dE/dX)_{\text{HI}}}{(dE/dX)_{\text{ep}}} = \frac{(\gamma_{\text{HI}}^2 Z_{\text{HI}}^2 Z_2 / v^2 A_2) \ln(2mv^2/I)}{(\gamma_p^2 Z_2 / v^2 A_2) \ln(2mv^2/I)} = \frac{\gamma_{\text{HI}}^2 Z_{\text{HI}}^2}{\gamma_p^2}, \quad (2)$$

where the HI and  $p$  subscripts denote heavy ions and protons, respectively.

<sup>9</sup> C. D. Moak and M. D. Brown, Phys. Rev. **149**, 244 (1966).

<sup>10</sup> M. S. Livingston and H. A. Bethe, Rev. Mod. Phys. **9**, 245 (1937).

Over most of the velocity region covered in this work, protons are completely ionized, and  $\gamma_p^2=1$ , yielding further simplification of Eq. (2). Where this was not the case, values of  $\gamma_p^2$  based on work by Hall, as reported by Booth and Grant, were used.<sup>4</sup> Also for a few points reported in this work, the experimental  $\Delta E/\Delta X$  values of Table I were reduced up to 5% for contributions due to nuclear stopping. For this purpose we used the asymptotic approximation<sup>11</sup>

$$(d\epsilon/d\rho)_n = (1/2\epsilon) \ln 1.294\epsilon, \quad (3)$$

where  $\epsilon$  and  $\rho$  are the dimensionless energy and range variables defined by Lindhard *et al.*,<sup>3</sup> and the subscript

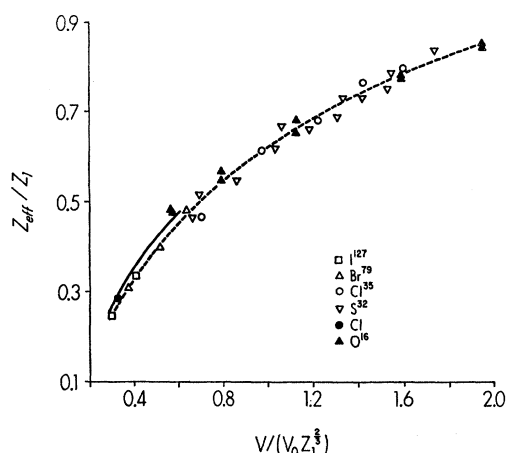


FIG. 1. Correlation of fractional effective charge versus reduced velocity. The ordinate and abscissa are the fractional effective charge  $\gamma_1$  and reduced velocity variables as defined in the text. Fractional effective charges based on the data of Table I are identified on the graph. The closed circles and closed triangles represent values calculated from the data of Ref. 4. The solid curve is taken from a similar correlation of fission fragments in Mylar in Ref. 3. The dashed curve is visually drawn to show the precision with which the fractional effective charges fall on a single smooth curve.

$n$  denotes nuclear stopping. Equation (3) extends the nuclear-stopping curve of Ref. 3 to higher  $\epsilon$  values than those of Ref. 3.

We then look for a correlation between "effective charge" calculated with Eq. (2) and the reduced velocity, assuming that the characteristics of the stopping medium at a given ion velocity are, to first order, removed by using the experimentally determined proton stopping powers<sup>12</sup> in that medium, as is implied by Eq. (2). If electrons having velocities less than the ion velocity are lost in collisions,<sup>13</sup> Eq. (2) should yield a consistent dependence of fractional effective charge  $\gamma_1 = Z_{\text{eff}}/Z_1$ , on the reduced velocity.

<sup>11</sup> J. Lindhard (private communication).

<sup>12</sup> W. Whaling, in *Handbuch der Physik*, edited by S. Flügge (Springer-Verlag, Berlin, 1958), Vol. 34, p. 193.

<sup>13</sup> N. Bohr, Kgl. Danske Videnskab. Selskab., Mat. Fys. Medd. 18, No. 8 (1948).

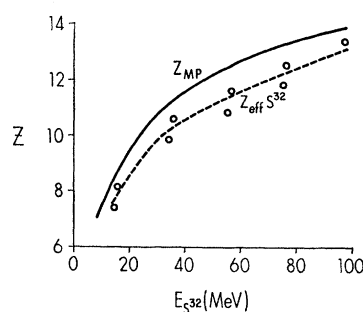


FIG. 2. Comparison of most probable and effective charges for  $S^{32}$  ions in Mylar. The solid curve represents the most probable charge ( $Z_{\text{MP}}$ ) as a function of kinetic energy ( $E_{S^{32}}$ ) for  $S^{32}$  ions in Formvar. Open points represent the effective charges of  $S^{32}$  ions in Mylar based on the stopping powers of Table I in conjunction with Eq. (2). The dashed curve was visually drawn through the effective-charge values.

The effective charges calculated with Eq. (2) for the  $\Delta E/\Delta X$  values of Table I are displayed in Fig. 1, as fractional effective charges. Also shown on Fig. 1 are fractional effective charge values for  $O^{16}$  ions on carbon and aluminum, and one point for Cl ions on carbon. It would appear that the correlation between the fractional effective charges and reduced ion velocities is within the experimental uncertainties in  $\Delta E/\Delta X$ . Fractional effective charges calculated for 20–100 MeV  $Br^{79,81}$  and  $I^{127}$  ions in Be, C, Al, Ni, Ag, and Au also fit the curves of Fig. 1 within experimental uncertainties.<sup>3,9</sup> Thus, the correlation seems to be independent of stopping medium for solids. The solid curve in Fig. 1 is the curve for fission fragments in Mylar of Ref. 3. An expression for the logarithmic factor of Eq. (1) was used in Ref. 3 rather than making a direct comparison with proton stopping powers. When proton stopping powers are used, an even better agreement with the data of this work results.

A comparison between the effective charge states extracted from Eq. (2) and the measured most probable equilibrium charge states is shown in Fig. 2 for  $S^{32}$  ions and in Table II for  $Br^{79}$  and  $I^{127}$  ions.<sup>14,15</sup> The most probable equilibrium charge states quoted do not differ

TABLE II. Comparison of effective and most probable charges for Br and I ions in Mylar.

Ion	Mean energy (MeV)	$Z_{\text{eff}}$	$Z_{\text{MP}}$
Br	90	16.8	19.6
	60	14.0	17.1
	31	10.9	14.3
I	105	17.8	26.6
	58	13.0	21.7

<sup>14</sup> H. D. Betz, G. Hortig, E. Leischner, Ch. Schmelzer, B. Stadler, and J. Weihrach, Phys. Letters 22, 643 (1966).

<sup>15</sup> F. Chmara, L. Grodzins, R. Kalish, and P. Rose, Bull. Am. Phys. Soc. 12, 479 (1967).

significantly from the rms values which technically should be used. The equilibrium charge states were measured for Formvar and carbon stripping foils; comparisons between charge states in different media imply that these values should not differ measurably from those in Mylar.<sup>14</sup> The same qualitative discrepancy between effective and rms charge states was noted in Ref. 3 for Br and I ions in various foils, and for Cl ions in gold and aluminum foils in Ref. 4. In the latter work, the effective charges of O<sup>16</sup> ions were found to agree within experimental uncertainties with the rms charge values in gold and aluminum. We can, at present, offer no explanation for the large discrepancies between effective charge and actual charge. The obvious empirical statements are that the effective charge of Eq. (2) must at present be considered solely as a parameter, and the rms charge values may not be used with Eq. (2) to calculate  $(dE/dX)_e$  for heavy ions.

The correlation of Fig. (1) implies the possibility of computing heavy-ion  $dE/dX$  values by estimating an effective charge from Fig. 1 and substituting this value and proton stopping powers into Eq. (2). While

the correlation is good in the higher-velocity region of Fig. 1 for O<sup>16</sup>, S<sup>32</sup>, and Cl<sup>35</sup> ions, the Br<sup>79</sup> and I<sup>127</sup> data do not extend into this region. It would, therefore, be valuable to have stopping-power data for higher-energy bromine and iodine ions in order to extend the range of ions and velocities over which the curve of Fig. 1 may be used to calculate stopping powers. The curve of Fig. 1 is also consistent with the results of Heckman *et al.* for lighter heavy ions.<sup>16</sup>

#### ACKNOWLEDGMENTS

The authors appreciate helpful discussions with Dr. J. B. Cumming and Dr. P. B. Price and correspondence with Professor J. Lindhard relevant to this work. The hospitality of Professor H. E. Gove and the staff of the Rochester Nuclear Structure Research Laboratory (supported by the National Science Foundation) is gratefully acknowledged. The authors wish to thank Dr. C. J. Heffelfinger of E. I. Dupont Company for providing the 335- $\mu$ g/cm<sup>2</sup> Mylar foils.

<sup>16</sup> H. H. Heckman, B. L. Perkins, W. G. Simon, F. M. Smith, and W. H. Barkas, *Phys. Rev.* **117**, 544 (1960).

### Mössbauer Studies of the SrTiO<sub>3</sub>:Fe<sup>57</sup> System

V. G. BHIDE AND H. C. BHASIN

*National Physical Laboratory, New Delhi, India*

(Received 16 January 1968; revised manuscript received 19 April 1968)

Mössbauer studies of the SrTiO<sub>3</sub>:Fe<sup>57</sup> system used as an absorber have shown that iron enters the SrTiO<sub>3</sub> lattice substitutionally at the Ti<sup>4+</sup> site in its high-spin ferric state and is usually associated with a charge-compensating oxygen vacancy in agreement with the EPR evidence. On firing these samples in hydrogen, the quadrupole-split spectrum of Fe<sup>3+</sup> associated with an oxygen vacancy transforms into a Zeeman-split spectrum with hf field and isomer shift characteristic of iron metal, indicating the formation of colloidal iron. Vacuum firing of the original air-fired samples tends to convert part of the Fe<sup>3+</sup> ions into Fe<sup>2+</sup> through the creation of more oxygen vacancies. The stages through which atomically dispersed Fe<sup>3+</sup> ions are converted into colloidal iron on hydrogen firing and vice versa have been indicated.

#### I. INTRODUCTION

THE EPR studies of Fe<sup>3+</sup> in SrTiO<sub>3</sub> reported by Müller<sup>1</sup> and Dobrov *et al.*<sup>2</sup> suggest that Fe enters the SrTiO<sub>3</sub> lattice at the Ti<sup>4+</sup> site in its high-spin ferric state without any vacancy association. These studies have been carried out with extremely low concentrations of iron. If, however, the concentration of iron is increased, there is a possibility for a charge-compensating oxygen vacancy to be associated with the probe, as is suggested by Mössbauer-effect (ME) studies of the BaTiO<sub>3</sub>:Fe<sup>57</sup> system.<sup>3</sup> Further, it has been shown by our earlier results that the valence state of a ME probe in a given lattice can be altered by giving any

of a variety of heat treatments to the system.<sup>4</sup> This paper reports the ME study of Fe-doped SrTiO<sub>3</sub> subjected to a variety of heat treatments. It is seen that for all the concentrations that are normally used in the ME studies, the Fe<sup>57</sup> probe in an air-fired SrTiO<sub>3</sub> system is associated with a charge-compensating oxygen vacancy. The reduction of the lattice by vacuum firing tends to stabilize the Fe<sup>2+</sup> state in addition to the usual Fe<sup>3+</sup> state. On firing the samples in hydrogen, however, colloids of iron have been detected, confirming once again that the electronic structure of the ME probe is dependent on the thermal treatment of the sample.

#### II. EXPERIMENTAL: SAMPLE PREPARATION

Single crystals of SrTiO<sub>3</sub> grown by the Verneuil technique were obtained from the National Lead Co.<sup>5</sup>

<sup>1</sup> K. A. Müller, *Helv. Phys. Acta* **31**, 173 (1958).

<sup>2</sup> W. I. Dobrov, R. F. Vieth, and M. E. Browne, *Phys. Rev.* **115**, 79 (1959).

<sup>3</sup> V. G. Bhide and M. S. Multani, *Phys. Rev.* **149**, 289 (1966).

<sup>4</sup> V. G. Bhide and H. C. Bhasin, *Phys. Rev.* **159**, 586 (1967).

<sup>5</sup> A batch of the single crystals was given by the National Lead Co., New York.